

Journal of Visualized Experiments

Human Ex Vivo Wound Model and Whole-Mount Staining Approach to Accurately Evaluate Skin Repair. --Manuscript Draft--

Article Type:	Invited Results Article - JoVE Produced Video
Manuscript Number:	JoVE62326R1
Full Title:	Human Ex Vivo Wound Model and Whole-Mount Staining Approach to Accurately Evaluate Skin Repair.
Corresponding Author:	Holly Wilkinson Hull York Medical School Hull, East Riding of Yorkshire and the Humber UNITED KINGDOM
Corresponding Author's Institution:	Hull York Medical School
Corresponding Author E-Mail:	h.n.wilkinson@hull.ac.uk
Order of Authors:	Holly Wilkinson Alexandria Kidd Elizabeth Roberts Matthew Hardman
Additional Information:	
Question	Response
Please specify the section of the submitted manuscript.	Developmental Biology
Please indicate whether this article will be Standard Access or Open Access.	Open Access (US\$4,200)
Please indicate the city, state/province, and country where this article will be filmed . Please do not use abbreviations.	Hull, United Kingdom
Please confirm that you have read and agree to the terms and conditions of the author license agreement that applies below:	I agree to the UK Author License Agreement (for UK authors only)
Please provide any comments to the journal here.	

TITLE:

Human Ex Vivo Wound Model and Whole-Mount Staining Approach to Accurately Evaluate Skin Repair

AUTHORS AND AFFILIATIONS:

Holly Nicola Wilkinson¹, Alexandria Sarah Kidd¹, Elizabeth Rose Roberts¹ and Matthew James Hardman¹

¹Centre for Atherothrombosis and Metabolic Disease, Hull York Medical School, University of Hull, HU6 7RX.

CORRESPONDING AUTHOR:

Holly N Wilkinson (h.n.wilkinson@hull.ac.uk)

EMAIL ADDRESSES:

Holly Nicola Wilkinson (h.n.wilkinson@hull.ac.uk)

Alexandria Sarah Kidd (Alex.Kidd@hull.ac.uk)

Elizabeth Rose Roberts (e.roberts@hull.ac.uk)

Matthew James Hardman (m.hardman@hull.ac.uk)

KEYWORDS:

wound healing, skin, human, ex vivo, whole-mount, staining, diabetes, aging, chronic wound

SUMMARY:

Here we demonstrate an optimized technique for assessing wound repair using ex vivo human skin combined with a whole-mount staining approach. This methodology provides a pre-clinical platform for the evaluation of potential wound therapies.

ABSTRACT:

Chronic non-healing wounds, which primarily affect the elderly and diabetic, are a significant area of clinical unmet need. Unfortunately, current chronic wound treatments are inadequate, while available pre-clinical models poorly predict the clinical efficacy of new therapies. Here we describe a high throughput, pre-clinical model to assess multiple aspects of the human skin repair response. Partial thickness wounds were created in human ex vivo skin and cultured across a healing time course. Skin wound biopsies were collected in fixative for the whole-mount staining procedure. Fixed samples were blocked and incubated in primary antibody, with detection achieved via fluorescently conjugated secondary antibody. Wounds were counterstained and imaged via confocal microscopy before calculating percentage wound closure (re-epithelialization) in each biopsy. Applying this protocol, we reveal that 2 mm excisional wounds created in healthy donor skin are fully re-epithelialized by day 4-5 post-wounding. On the contrary, closure rates of diabetic skin wounds are significantly reduced, accompanied by perturbed barrier reformation. Combining human skin wounding with a novel whole-mount staining approach allows a rapid and reproducible method to quantify ex vivo wound repair. Collectively, this protocol provides a valuable human platform to evaluate the effectiveness of

potential wound therapies, transforming pre-clinical testing and validation.

INTRODUCTION:

Chronic, non-healing wounds, which are highly prevalent in the elderly and diabetic, are a majorly unappreciated area of clinical unmet need. These wounds present a major physical and psychological burden to patients and cost healthcare providers billions each year to treat¹. Despite improved understanding of wound biology and advancements in technology, up to 40% of chronic wounds still fail to heal following best standard care². Thus, 14-26% of patients with diabetic foot ulcers subsequently require amputation³, while 5-year post-amputation mortality rate stands at approximately 70%⁴. As a result, there is an urgent requirement to develop efficacious new therapies to improve patient quality of life while reducing the substantial healthcare burden imposed by poor healing wounds. Poorly predictive pre-clinical models remain a significant hurdle to the development of effective new therapies.

Wound repair is a dynamic and multifaceted process involving a diverse range of cell types, countless levels of communication and a tissue environment that is temporally remodeled. Skin healing is underpinned by four major reparative stages: hemostasis, inflammation, proliferation, and matrix remodeling. These stages ultimately act to prevent blood loss and infection, close the wound surface (a process termed re-epithelialization) and return the skin to an uninjured state⁵. Chronic wounds are associated with diverse etiology and widespread perturbation to healing processes⁶, further complicating the identification of therapeutic targets. Nevertheless, a broad range of models have been developed to both elucidate the molecular and cellular drivers of wound pathology and test new therapeutic approaches⁷.

The most used wound repair model is acute wounding in the mouse. Mice are highly tractable for mechanistic studies and provide validated models of ageing and diabetes⁸. Despite the general similarities shown amongst mouse and human healing, between-species differences in skin structure and healing dynamics remain. This means most murine wound research does not easily translate to the clinic⁹. Consequently, there has been a push towards human in vitro and ex vivo systems with high applicability and translatability^{10,11}.

Here we provide an in-depth protocol for performing partial thickness excisional wounds in ex vivo human skin. We, also, outline our whole-mount staining approach as a highly reproducible method of evaluating ex vivo human skin healing. We show the trajectory of epidermal repair (re-epithelialization) and subsequent barrier formation, evaluating the rate of wound closure in healthy versus diabetic human skin. Finally, we demonstrate how whole-mount staining can be adapted for use with a range of antibodies to assess various aspects of the healing response.

PROTOCOL:

Human skin was obtained from patients undergoing reconstructive surgery at Castle Hill Hospital and Hull Royal Infirmary (Hull, UK) under full informed, written patient consent, institutional guidelines, and ethical approval (LRECs: 17/SC/0220 and 19/NE/0150). Non-diabetic skin was collected from patients undergoing routine surgery (mean age = 68). Diabetic skin was selected from donors who had established type II diabetes and a history of ulceration (mean age = 81).

Samples from surgery were transported in holding media and processed immediately upon arrival at the laboratory. All experimental steps using unfixed human tissue were performed at Biosafety Level-2 (BSL-2) in a class II laminar flow biosafety cabinet.

1. Preparation of skin culture media and staining reagents

NOTE: All reagent and consumable details are provided in the **Table of Materials**. Ensure all reagents and equipment used for the processing and culture of human tissue are sterile. Sterilize instruments prior to the use and decontaminate with disinfectant following contact with the tissue. Decontaminate waste products in 1% disinfectant before disposal.

1.1. Holding media: Supplement high glucose Dulbecco's Modified Eagle Medium (DMEM) with 2 mM L-glutamine and 4% (v/v) antibiotic-antimycotic solution.

1.2. Hank's balanced salt solution (HBSS) with antibiotics: Add 4% (v/v) antibiotic-antimycotic solution to HBSS. Store at 4 °C until use.

1.3. Dulbecco's phosphate buffered saline (DPBS): Prepare DPBS by dissolving 9.6 g of DPBS powder per liter of distilled water (dH₂O). Autoclave to sterilize and store at 4 °C until use.

1.4. Human skin growth media: Supplement high glucose DMEM with 2 mM L-glutamine, 1% (v/v) antibiotic-antimycotic solution and 10% (v/v) fetal bovine serum. Store at 4 °C until use.

1.5. Skin fixative: To 450 mL of dH₂O, add 40 mL of formaldehyde solution, 10 mL of glacial acetic acid, 4.5 g of sodium chloride and 0.25 g of alkyltrimethylammonium bromide. Store at room temperature (RT) and use within a few days.

CAUTION: Fixative is hazardous (irritant and flammable). Handle with care and dispose of via an appropriate route.

1.6. Phosphate buffered saline (PBS): Prepare PBS for whole mount staining by adding 6 g of sodium chloride to 100 mL of phosphate buffer solution and 900 mL of dH₂O.

1.7. Staining wash buffer: Dissolve 0.5% (v/v) Triton X-100 in PBS.

1.8. Blocking buffer: Add 0.2% (w/v) sodium azide and 2% (v/v) animal serum to staining wash buffer. Store at 4 °C for up to two weeks.

NOTE: Block in the serum of the secondary antibody host species. Sodium azide will prevent bacterial growth during incubation.

1.9. DAPI working solution: Prepare a 5 mg/mL stock of 4',6-diamidino-2-phenylindole (DAPI) in dimethyl sulfoxide. Dilute the stock 1:1,000 in staining wash buffer to give a 5 µg/mL DAPI working solution.

1.10. Peroxidase block: Add 0.3% (v/v) hydrogen peroxide to staining wash buffer. Store at 4 °C until use. Keep in the dark to prevent decomposition.

1.11. ABC-HRP Kit:

1.11.1. HRP-conjugated secondary antibody: 1 drop of biotinylated rabbit anti-goat IgG in 5 mL of staining wash buffer. Store at 4 °C for up to two weeks.

NOTE: The kit/secondary used will depend on the host species of the primary antibody.

1.11.2. Avidin-biotin complex (ABC) reagent: 2 drops of reagent A and 2 drops of reagent B in 5 mL of staining wash buffer. ABC reagent should be prepared at least 30 min prior to use. Store at 4 °C for up to two weeks.

1.12. Peroxidase substrate: 3 drops of reagent 1, 2 drops of reagent 2, 2 drops of reagent 3 and 2 drops of hydrogen peroxide in 5 mL of dH₂O. Peroxidase substrate should be freshly prepared immediately before use and cannot be stored.

2. Preparation of skin for wounding

NOTE: These steps should be performed in a class II laminar flow biosafety cabinet.

2.1. Collect the skin in holding media and transport to the BSL-2 cabinet.

2.2. Place the skin dermis side down within a 90 mm sterile Petri dish and remove adipose tissue with sterile scissors.

2.3. Place the skin in a 50 mL tube containing 25 mL of HBSS with antibiotics for 10 min at RT. Shake intermittently to remove any residual blood and adipose tissue.

2.4. Repeat step 2.3 using a new 50 mL tube.

2.5. Place the skin in a fresh 50 mL tube containing 25 mL of HBSS, this time without antibiotics for 10 min at RT. Shake as in step 2.3.

2.6. Perform a final skin rinse by placing skin in a new tube with 25 mL of DPBS. The skin is now ready to wound.

3. Creating ex vivo human skin wounds

NOTE: These steps should be performed in a class II laminar flow biosafety cabinet.

3.1. Prepare the skin culture dishes prior to wounding. In a 60 mm Petri dish, stack two sterile

absorbent pads and add 4 mL of human skin media via the side of the dish. Place a sterile nylon filter membrane onto the absorbent pad stack.

NOTE: Skin media can be altered depending on the required treatment conditions. Up to three wound explants may be cultured on each stack.

3.2. Dry the dermal side of the skin on sterile gauze in a 90 mm Petri dish to remove residual DPBS.

NOTE: This prevents the skin from sliding around when wounding.

3.3. Place the skin dermis side down on a clean 90 mm Petri dish lid and dab the epidermis dry with fresh sterile gauze.

NOTE: It is easier to wound the skin in a Petri dish lid than the base. Subsequent work should be carried out quickly to prevent the skin drying out.

3.4. Holding the skin taut, press a 2 mm biopsy punch against the skin and twist gently. Do not punch entirely through the skin.

NOTE: Partial thickness wounds are designed to punch through the epidermis and partially into the dermis. There may be donor-to-donor and site-to-site variability in the force required to create the partial thickness wound.

3.5. Use curved toothed tissue forceps to pick up each side of the 2 mm wound and hook curved iris scissors under the 2 mm wound to cut it out uniformly.

3.6. Biopsy around the central 2 mm wound using a 6 mm biopsy punch to create a 6 mm explant with a partial thickness 2 mm wound in the center.

NOTE: A 6 mm biopsy punch may be used to score the skin to mark out where each 2 mm wound should be. Take care not to pierce through the tissue entirely. Create wound explants in a honeycomb pattern to reduce wastage.

3.7. Place wound explants epidermis side up on the nylon filter membrane stack (prepared in step 3.1).

NOTE: When handling wound explants, be careful not to damage the central wound. Use small forceps and pick up each explant at opposite sides.

3.8. Incubate wounds at 32-37 °C and 5% CO₂ in a humidified atmosphere (90-95%) for 1-7 days. Replace the media every 2-3 days.

4. Whole mount staining of ex vivo wounds

NOTE: This section describes immunofluorescence and immunoperoxidase staining methods. Mix all reagents well before use.

4.1. Fluorescent staining method

4.1.1. Collect wound explants in 1.5 mL microcentrifuge tubes containing 500 μ L of skin fixative and incubate at 4 °C overnight.

NOTE: The fixative used in this protocol works well for the described antibodies. Optimization will be required for other antibodies. Tissue fixation longer than 24 h may lead to over-fixation.

4.1.2. The following day remove the fixative and replace with 1 mL of staining wash buffer. Biopsies can be stored in staining wash buffer at 4 °C up to 2 weeks prior to staining.

NOTE: For all wash buffer steps, use a serological pipette or pipette tip, taking care not to damage the wound.

4.1.3. Aspirate the staining wash buffer and perform one more rinse with 1 mL of staining wash buffer.

4.1.4. Calculate the amount of blocking buffer required for steps 4.1.5-4.1.6 (number of samples x 300 μ L = amount of blocking buffer in μ L). Make extra buffer if required.

4.1.5. Add 150 μ L of blocking buffer to each sample and incubate for 1 h at RT. For all staining steps, ensure each sample is sufficiently covered and that there are no bubbles covering the biopsy wound surface.

NOTE: This step onwards can be performed in 1.5 mL microcentrifuge tubes or in a 48 well plate. If using a 48 well plate, incubate the wounds face down in each well.

4.1.6. Dilute the primary antibody in the remaining blocking buffer.

NOTE: Anti-mouse keratin 14 (K14) diluted 1:1,000 in blocking buffer works well. Optimize this step for use with other antibodies or multiple probes.

4.1.7. Aspirate the blocking buffer and add 150 μ L primary antibody per well/microcentrifuge tube. Incubate wound explants in primary antibody at 4 °C overnight.

4.1.8. The next day, aspirate the primary antibody and rinse in staining wash buffer containing 0.2% sodium azide for 1 h at RT (500 μ L per sample).

4.1.9. Perform three more rinsing steps using staining wash buffer (30 min per wash, 500 μ L per sample).

265
266 4.1.10. Dilute the fluorescently conjugated secondary antibody in staining wash buffer (e.g., goat
267 anti-mouse 488 at 1:400 dilution).

268
269 4.1.11. Calculate the required amount of secondary antibody (number of samples x 150 μ L =
270 amount in μ L).

271
272 4.1.12. Add 150 μ L of secondary antibody to each well/microcentrifuge tube. Incubate for 1 h at
273 RT. Perform incubation steps 4.1.10 – 4.1.16 in the dark as the secondary antibody is light
274 sensitive.

275
276 NOTE: This step can be performed at 4 °C overnight if required. Optimize the concentration of
277 secondary antibody required for adequate signal and limited background staining.

278
279 4.1.13. Remove the secondary antibody and perform 3 x 30 min rinses with staining wash buffer
280 (500 μ L per sample).

281
282 4.1.14. Discard the leftover wash buffer and calculate the amount of DAPI working solution
283 required (as per step 4.1.11).

284
285 4.1.15. Counterstain each explant with 150 μ L of DAPI working solution for 10 min at RT.

286
287 NOTE: DAPI will stain cell nuclei blue. Hoechst dye can be used as an alternative to DAPI.

288
289 4.1.16. Perform two final 30 min washes with staining wash buffer (500 μ L per sample). Biopsies
290 can be stored in staining wash buffer at 4 °C in the dark up to two weeks prior to imaging.

291
292 4.2. Brightfield staining method.

293
294 4.2.1. Perform steps 4.1.1 – 4.1.3.

295
296 4.2.2. Quench endogenous peroxidase activity with peroxidase block at 4 °C overnight.

297
298 NOTE: This step is important when using an HRP-conjugated antibody to reduce non-specific
299 background staining from the tissue. Highly vascularized tissue will contain more endogenous
300 peroxidase activity.

301
302 4.2.3. Discard the peroxidase block and rinse twice for 30 min in staining wash buffer.

303
304 4.2.4. Perform steps 4.1.4 – 4.1.8.

305
306 NOTE: Washes after step 4.1.7 are particularly important to remove sodium azide from the
307 samples. If sodium azide is not adequately removed, it will inactivate the HRP and interfere with
308 staining detection.

4.2.5. Add 150 μ L HRP-conjugated secondary antibody to each well/microcentrifuge tube and incubate overnight at 4 $^{\circ}$ C or 1 h at RT.

4.2.6. Remove the secondary antibody and perform 3 x 30 min washes in staining wash buffer.

4.2.7. Add 150 μ L ABC reagent to each well/microcentrifuge tube and incubate overnight at 4 $^{\circ}$ C or 1 hour at RT.

4.2.8. Aspirate the ABC reagent and perform 3 x 30 min washes in staining wash buffer.

4.2.9. Add 150 μ L peroxidase substrate to one explant and determine the time required to detect a noticeable color change.

NOTE: Choose a sample where strong staining is expected. In this case, a red ring to show the migrating epidermis (K14). 3,3'-diaminobenzidine-4, or any other appropriate chromogenic substrate, may be used as a replacement for this peroxidase substrate.

4.2.10. Once a color change is observed, remove the peroxidase substrate, and replace with 1 mL of dH₂O.

4.2.11. Repeat the peroxidase substrate detection for the other explants, incubating for the time determined in step 4.2.11.

4.2.12. Rinse all explants with 1 mL of dH₂O to remove residual peroxidase substrate. Although explants may be stored up to one week at 4 $^{\circ}$ C prior to imaging, it is better to image them as soon as possible to prevent leaching of the peroxidase substrate into the dH₂O over time.

5. Imaging and quantification

5.1. Fluorescent imaging

NOTE: Fluorescent imaging is performed using a confocal laser-scanning microscope. However, an inverted fluorescent microscope may be sufficient for acquiring 2D images to quantify wound closure rates. When selecting secondary antibodies, ensure that the chosen fluorochromes are compatible with the excitation and emission spectra of the microscopy equipment available.

5.1.1. Use a confocal laser-scanning microscope equipped with a 2.5x, 10x and 20x objective, x-y-z motorized stage, digital camera, and acquisition software. Switch on the transmitted light detector (TPMT) to allow easy visualization of each biopsy and to enable measurement of total wound closure. Alternatively, measure each wound via brightfield microscopy following fluorescence imaging.

5.1.2. Place a 60 mm Petri dish base on the imaging platform and add a thin layer (around 1 mL)

of DPBS.

NOTE: If too much DPBS is used, the biopsy will move around during imaging. Alternatively use a 48 well plate if a plate holder is available.

5.1.3. Use small tissue forceps to transfer wound explants from wells/microcentrifuge tubes to the Petri dish containing DPBS. Place the wound side down in the Petri dish.

5.1.4. Use the eyepiece and fluorescent lamp to locate and focus on the wound. If bubbles are trapped under the sample in the field of view, pick up the wound with tissue forceps and reposition.

5.1.5. Set up the imaging software, ensuring equal pinhole size between channels for optimum confocality. For this, check the value of one airy unit for each channel and select the largest value. Select scan speed, image quality and averaging.

NOTE: The fluorochromes of the conjugated secondary antibodies and the chosen counterstain (e.g., DAPI) will dictate the channels required.

5.1.6. Switch on the live acquisition software and adjust the laser power and gain of each channel to the levels required to visualize staining. Reduce background noise by increasing the digital offset.

5.1.7. Position the wound in the center of the imaging plane.

NOTE: If the wound does not fill the entire image due to using a smaller objective or creating a larger wound, take a panel of images and stitch them together (manually or with a tiling function in the relevant imaging software).

5.1.8. Acquire images of the wound biopsies. Use the same imaging settings between explants.

NOTE: Higher power images will allow assessment of tissue structures and cellular marker expression and location.

5.1.9. Collect serial Z stacks through the wound, especially where the tissue is not completely flat against the Petri dish. Use analysis software to collapse the Z stack into a single maximum intensity projection image.

5.2. Brightfield imaging

NOTE: Brightfield imaging of immunoperoxidase stained biopsies can be performed in multiple ways.

5.2.1. Inverted microscope imaging: Prepare wound explants for imaging by placing them in a

Petri dish/well as described in steps 5.1.2-5.1.3. Acquire digital images under brightfield illumination on an inverted microscope equipped with a digital camera. Stitch together multiple images if required.

5.2.2. Wireless digital microscope imaging: Use a wireless digital microscope connected to a phone or laptop to obtain high quality images in a cost-effective manner. Place explants wound side up onto some tissue and remove any residual dH₂O (or staining wash buffer) from sample storage. Position the wound explant in the center of the microscope field of view. Acquire images using the connected camera.

5.3. Quantification

NOTE: Percentage wound closure can be quantified in any software that allows freehand shapes to be drawn and measured. ImageJ can be used to perform quantification as follows:

5.3.1. Open the image to be quantified in ImageJ software.

5.3.2. Use the freehand shape tool to draw around the outside of the re-epithelialized wound where it meets the normal skin. Press **M** (or **Analyze | Measure**) to acquire an 'outer' area measurement.

NOTE: The re-epithelialized wound tissue texture differs from normal skin. The images do not need to be scaled prior to this type of analysis.

5.3.3. Use the freehand shape tool to draw around the open wound area. This is where the open wound meets the inside edge of the re-epithelializing tissue. Press **M** (or **Analyze | Measure**) to acquire an 'inner' area measurement.

5.3.4. Use the following equation to deduce percentage wound re-epithelialization/closure:

$$\% \text{ Closure} = (\text{Outer wound area} - \text{Inner wound Area}) / (\text{Outer wound Area}) \times 100$$

NOTE: Percentage area coverage of antibodies can be deduced in the same way (e.g., K14) or as a percentage of the total wound area. Percentage intensity can also provide semi-quantitative information about tissue level expression of markers of interest, while high power imaging presents expression data at the cellular level.

RESULTS:

In this report, we present a novel ex vivo skin wounding and whole-mount staining approach to assess factors that influence the human skin repair response. **Figure 1A** shows a schematic of the procedural pipeline, which can be performed in 3-10 days, depending on wound incubation times. The partial thickness wounds are cultured on membrane stacks at the air : membrane interface and can be collected for whole-mount staining, embedded in paraffin or OCT medium

for general histology, or frozen in liquid nitrogen for biochemical analysis (**Figure 1B**). We generally create 2 mm partial thickness wounds within the center of 6 mm explants. However, the size of the wound and surrounding explant may be altered depending on requirements. The whole-mount procedure has been successfully adapted for both immunoperoxidase and immunofluorescence staining methods (**Figure 1C**).

Immunofluorescence allows for the probing of tissue with multiple antibodies. For this, we advise using primary antibodies raised in different species, and species-matched fluorescently conjugated secondary antibodies to limit cross-species reactivity. Antibody concentrations and incubation times will need to be optimized. If background staining is observed, reduce antibody concentrations, increase wash steps, and add blocking buffer to the secondary antibody. Fresh tissue viability can be directly assessed with commercial viability dyes (see **Table of Materials**). We also show that tissue may be fixed post viability staining and successfully imaged when it is practically suitable (**Figure 1D**).

[Place **Figure 1** here]

The most widely applicable use for whole mount staining of wounds is to determine wound closure rate in a more reproducible manner than can be provided via histological sectioning. Percentage closure was quantified as percentage re-epithelialization of the wound surface, as demonstrated in **Figure 2A**. Percentage area coverage of specific markers can be measured from the total wound area or as a percentage of the re-epithelialized wound. We characterized healing in healthy (non-diabetic) versus diabetic skin across a time course of seven days, collecting wounds at each day post-wounding (representative images, **Figure 2B**). Healthy skin wounds closed over time as expected, with full closure observed in most samples by day 4-5. On the contrary, diabetic skin wounds failed to close fully within the seven-day analysis period (**Figure 2C**). A significant delay in wound closure was observed between healthy and diabetic skin wounds when comparing healing rates at each time-point post-injury ($P < 0.001$ to day 6, $P < 0.05$ at day 6 and $P < 0.05$ to $P < 0.001$ at day 7).

Following assessment of overall wound closure rates; we measured the percentage of the entire wound area (outer area in **Figure 2A**) where K14 positive cells could be visualized (green staining in **Figure 2B**). Interestingly, we observed that in healthy ex vivo skin wounds, K14 staining peaked at day 2 and then rapidly declined (significance at each time-point versus the day 2 peak, **Figure 2D**). This is likely reflecting re-formation of the early epidermal barrier, excluding K14 antibody penetration through differentiated epidermal layers (see **Figure 2E** schematic). During the re-epithelialization process, basal layer (K14+ve) keratinocytes migrate inwards over the open wound such that the epidermis closer to the outer wound edge forms earlier than the epidermis closer to the inner wound edge (migrating front). While the front edge of the newly formed epidermis continues to migrate to close the remaining open wound, the outer edge epidermis begins to differentiate to reform the other epidermal layers. In early healing, we would thus expect to see most of the re-epithelialized area consists of basal (K14+ve) cells, while in later repair K14 staining is lost as the epidermis differentiates from the outside inwards (see whole-mount images in **Figure 2E**). Therefore, the decline in K14 staining shown in **Figure 2D** (downward

arrows) correlates with increased epidermal differentiation. Interestingly, visible K14 staining peaked earlier in healthy (day 2) versus diabetic (day 4) wounds, further demonstrating that re-epithelialization and subsequent epidermal differentiation are delayed in diabetic skin wounds.

[Place **Figure 2** here]

We next used whole-mount staining to explore tissue expression and localization of other wound-relevant markers in non-diabetic skin (**Figure 3**). All antibodies used and their working concentrations are provided in the **Table of Materials**. Blood vessels in the open wound stained positively with alpha smooth muscle actin (α -SMA) antibody, used in combination with K14 to delineate the epidermal edges in lower power images (**Figure 3A**). The dermal matrix was stained with antibodies against collagen type I (COL 1) and fibronectin (Fn). Here collagen was observed as abundant thick fibers while fibronectin fibers were sparse, wavy, and thin (**Figure 3A**). Our whole-mount staining approach is also able to provide cell level resolution of staining, as demonstrated for K14-positive keratinocytes (**Figure 3B**).

Finally, we show that human *ex vivo* wounds possess resident immune cells, with Langerhans cells detected around newly formed epidermis at day 3 post-wounding (**Figure 3C**). Indeed, these results suggest that whole-mount staining may be used to investigate key features of the healing response including inflammation, proliferation, and the extracellular matrix (**Figure 4A**). Taken together, our data reveal that the combined *ex vivo* skin wounding and whole-mount staining procedure is a valid method to assess various aspects of healthy and diabetic (pathological) human skin repair.

[Place **Figure 3** and **Figure 4** here]

FIGURE AND TABLE LEGENDS:

Figure 1: The human *ex vivo* wounding and whole-mount staining approach. (A) Pipeline depicting the procedural workflow from collecting skin and performing *ex vivo* wounding, to staining tissue and analyzing data. (B) Diagram demonstrating the human *ex vivo* skin wound culture system with analyses routinely performed on the tissue. (C) Whole-mount staining can be employed using both immunoperoxidase and immunofluorescence techniques. K14 = keratin 14. (D) Live tissue may be stained with commercial viability dyes and imaged successfully post fixation. Bar = 100 μ m. This staining was performed in non-diabetic skin.

Figure 2: Whole-mount staining reveals perturbed healing rates in diabetic versus healthy skin. (A) The method used to quantify wound closure from outer and inner wound measurements. Brightfield images show keratin 14 (K14) staining in red. Bar = 300 μ m. (B) Representative images of healing over time (day post-wounding) in healthy and diabetic skin. Bar = 500 μ m. K14 = green. DAPI = blue nuclei. (C) Quantification of wound closure rates (percentage re-epithelialization) showing that *ex vivo* wounds from healthy skin close significantly faster than *ex vivo* wounds from diabetic skin. H = healthy. Db = diabetic. (D) Percentage K14 staining peaks earlier in healthy versus diabetic skin and then declines in line with increased epidermal differentiation (down arrows). (E) K14 (basal epidermal cell) staining is lost as the epidermis differentiates. D =

differentiated. ND = not differentiated. White dotted lines depict inner and outer wound edges. White arrows = direction of migration. n = 6 wounds per donor, per time point. Mean +/- SEM. * = $P < 0.05$, ** = $P < 0.01$ and *** = $P < 0.001$. Healthy and diabetic compared at each healing time point in **C** (P value for least significant comparison). Temporal change in K14 staining compared to peak for each donor in **D**.

Figure 3: Optimization of the whole-mount staining approach for use with other antibodies. (A) Blood vessels were stained with alpha smooth muscle actin (α -SMA, green) and keratin 14 (K14, red), while matrix fibers were stained with collagen I (COL 1, red) and fibronectin (Fn, green). (B) The whole-mount procedure provides up to cell level resolution of localization (K14, green; K1, red). (C) CD1a+ve Langerhans cells (green) observed in newly formed epidermis. DAPI = blue nuclei. Bar = 100 μ m. White dotted lines show inner and outer wound edges and separate wound from epidermis. This staining was performed in non-diabetic skin.

Figure 4: Validity of the whole-mount staining procedure for assessing wound healing. (A) Illustration depicting how the whole-mount staining technique can evaluate wound-relevant processes. Antibodies used = red text. K14 = keratin 14. COL 1 = collagen 1. Fn = fibronectin. (B) The whole-mount staining procedure (blue arrows) introduces less variability to wound closure measurements than standard histological analysis (red arrows). S1 = section 1. WE = wound edge. Bar = 300 μ m. This staining was performed in non-diabetic skin.

DISCUSSION:

In this experimental protocol, we describe an optimized method for evaluating wound closure in human ex vivo skin using whole-mount tissue staining. This is an important resource to allow critical evaluation of potential wound treatments, and to provide better understanding of the human wound repair response. We have published healing assessment in ex vivo skin wounds previously^{12,13}, yet in these reports the whole-mount staining approach was not used to measure wound closure. Whole-mount staining is far easier and requires less technical experience than standard histology, which involves paraffin or OCT embedding and sectioning of samples. The whole-mount procedure also reduces experimental variability, allowing quantification of the entire wound and not just a single transverse section at a defined position within the tissue (see **Figure 4B** for comparative illustration). We fully support the importance of quantifying healing of the entire non-symmetrical wound structure, as clearly outlined by Rhea and Dunnwald for murine acute wounds¹⁴. These authors showed the importance of serially sectioning in vivo excisional wounds for reproducible and precise measurements of wound morphology. Serial sectioning could equally be applied to human ex vivo wounds; however, for accurate quantification of wound closure and re-epithelialization, high throughput whole-mount staining should be the preferred method. We note that this whole-mount staining protocol should also be compatible with subsequent processing (wax or OCT) for traditional histological analysis.

Whole-mount staining is not without disadvantages. While it affords higher reproducibility in wound healing experiments, it does require the use of more tissue for analysis than standard histological techniques. This may be an issue where tissue access is limited, particularly where multiple antibodies need to be assessed. An alternative approach would be to employ an

incisional wounding method where wound width is relatively uniform and variability is reduced (as shown in mouse and human wounds^{15,16}). However, excisional wounds remain more applicable to most pathological wound types¹⁷.

In this study, 2 mm partial thickness wounds were created within the center of 6 mm skin explants. This method may be optimized for alternative excisional wound and explant sizes at different skin depths¹⁸. In addition, the force required to generate wounds will vary between donors, where aged skin will require less force to biopsy. We would also avoid using skin displaying prominent stretch marks or other structural alterations. We have validated a range of antibodies to consider different aspects of the *ex vivo* healing response. This protocol may also be used with other skin-relevant antibodies, where antibody concentrations and incubation times will need to be optimized. Nevertheless, we believe our protocol is most suited to absolute quantification of total wound closure, followed by spatial assessment of specific proteins of interest. While whole mount provides reduced resolution of immunolocalization versus standard histological analysis of tissue sections, it provides additional 3D information that is missing from standard 2D histology.

One caveat of assessing healing in *ex vivo* skin versus *in vivo* models is that it lacks a systemic response. An important aspect of wound repair is inflammation and subsequent tissue granulation, which is caused by an influx of inflammatory cells and endothelial cells from the vasculature¹⁹. Despite this limitation, *ex vivo* skin still provides a better recapitulation of clinical healing than cell-based wound assays. *In vitro* experiments in general involve single cell type monolayers or co-cultures grown on tissue culture plastic, whereas *ex vivo* skin provides a native environment to explore cell behavior. More recently, a number of skin equivalent systems have emerged, where skin is grown in a laboratory setting from artificial matrix and isolated skin cells^{20,21}. Although these models mimic human skin better than most *in vitro* approaches, they still do not fully simulate the native tissue environment and are generally too fragile to injure reproducibly. Additionally, we (and others) have demonstrated that *ex vivo* human skin tissue retains resident immune cells, which will no doubt contribute to repair^{22,23}. Future work should now focus on extending the viability and immunocompetency of the *ex vivo* model for late-stage healing assessment²⁴. One option is further advancement of promising organ-on-a-chip technologies capable of prolonging tissue viability and maintaining native skin architecture for up to two weeks in culture²⁵. *Ex vivo* models have also begun to consider the importance of the skin inflammatory response by successfully incorporating immune cells, such as neutrophils, into the host tissue²⁶ or injecting host tissue with antibodies to elicit an immune reaction²⁷. We expect that these findings will pave the way for development of more refined and translatable methods in the future.

A major benefit of using *ex vivo* skin to measure wound closure is the ability to compare healing rates in healthy (e.g., non-diabetic) versus pathological (e.g., diabetic or aged) tissue. Here we showed that re-epithelialization and barrier formation are indeed impaired in diabetic versus healthy *ex vivo* wounds. Indeed, this provides a route for pre-clinical assessment of pathological repair, where ageing and diabetes are major risk factors for developing chronic wounds¹. While *in vitro* pathological models exist, such as cells isolated from aged and diabetic tissue, or cells

cultured in high glucose to mimic hyperglycemia^{28,29}, these cells can quickly lose their phenotype once removed from the in vivo microenvironment. An important component of the extrinsic pathological healing environment is the dermal matrix, which is altered in both ageing and diabetes³⁰. Indeed, this perturbed matrix affects the behavior of resident and naïve fibroblasts^{31,32}. Thus, the importance of studying cells in their host tissue environment cannot be underestimated.

In summary, our protocol provides an important platform to quantify human wound re-epithelialization, explore regulatory factors and to test the validity and efficacy of potential therapeutics^{12,13}. While pre-clinical testing does still require in vivo approaches, a combined strategy using ex vivo human tissue and in vivo murine wounding should refine the pre-clinical pathway, reducing animal use while increasing cross-species translatability.

ACKNOWLEDGMENTS:

We would like to thank Mr Paolo Matteuci and Mr George Smith for providing patient tissue. We are also grateful to Miss Amber Rose Stafford for assisting with tissue collection and the Daisy Appeal for providing laboratory facilities.

DISCLOSURES:

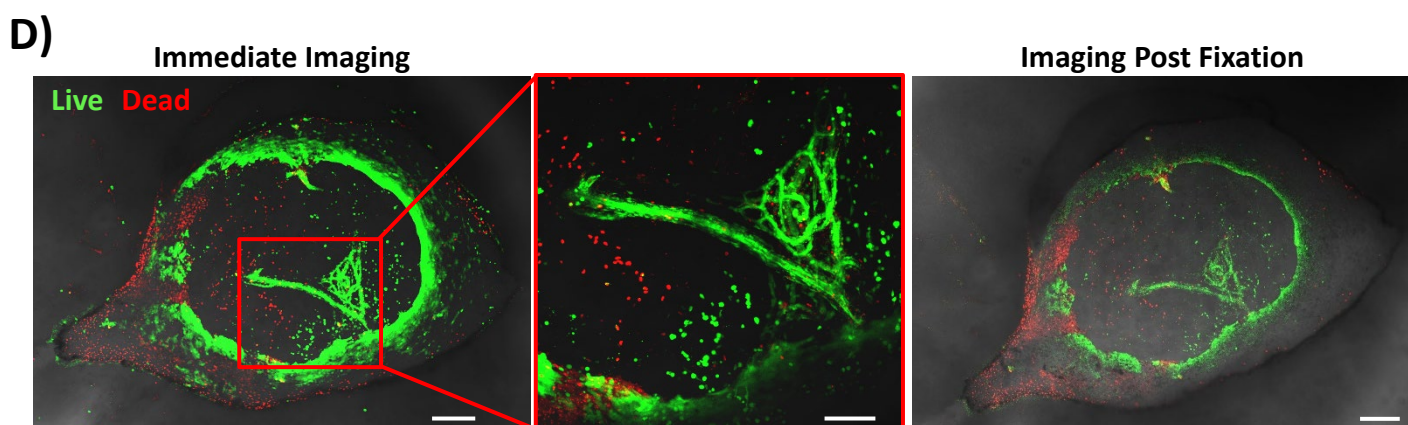
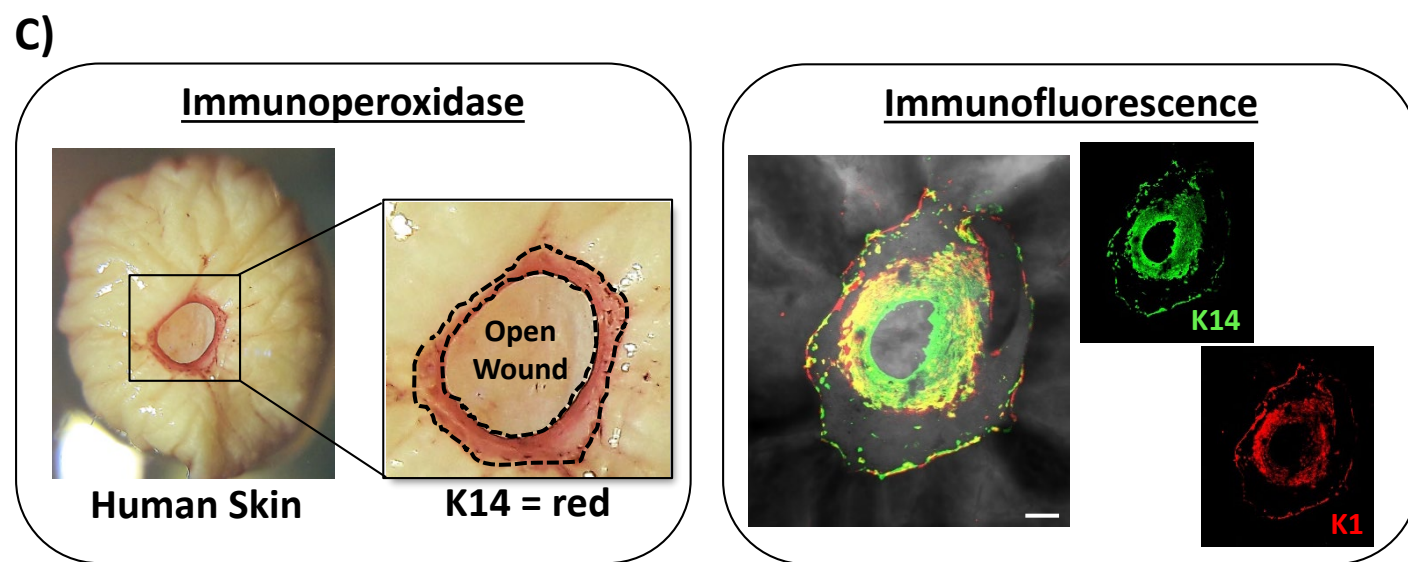
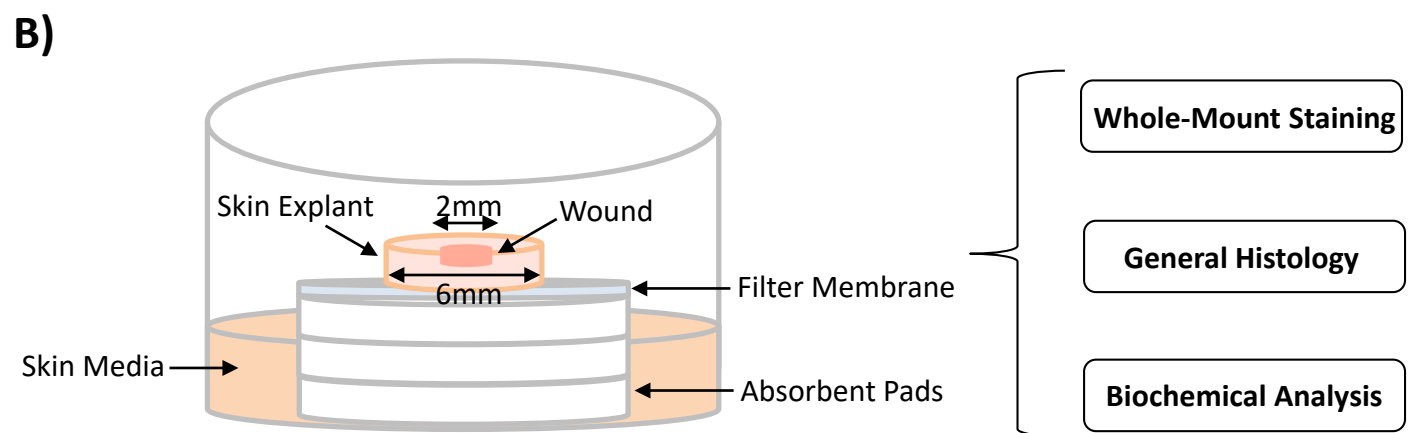
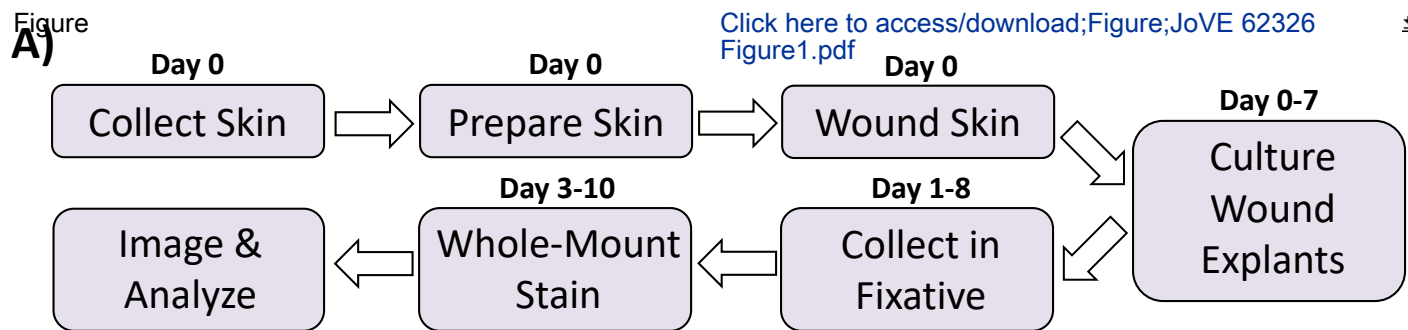
The authors declare no conflicts of interest.

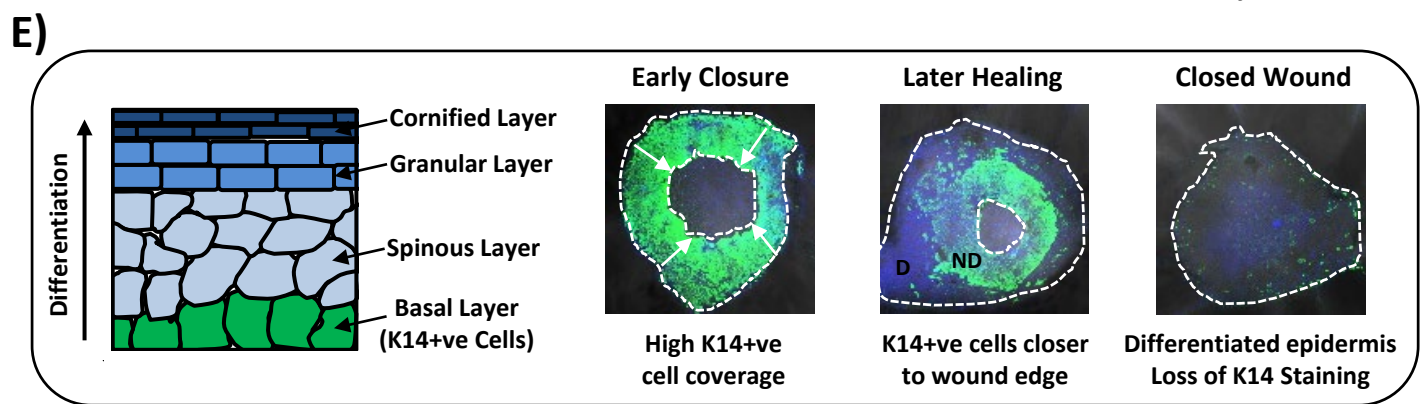
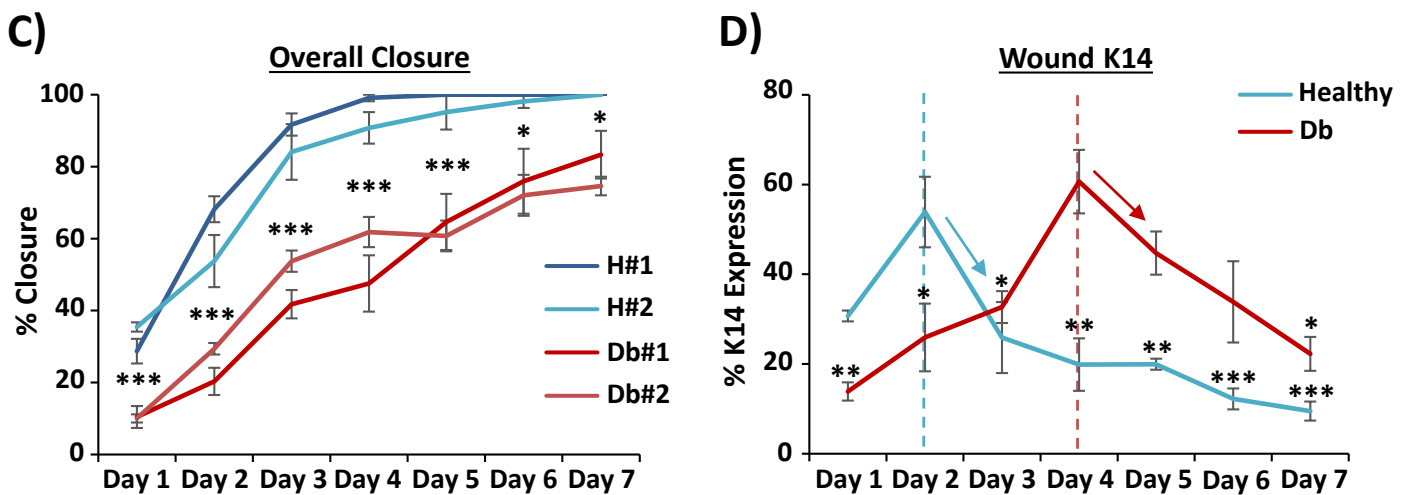
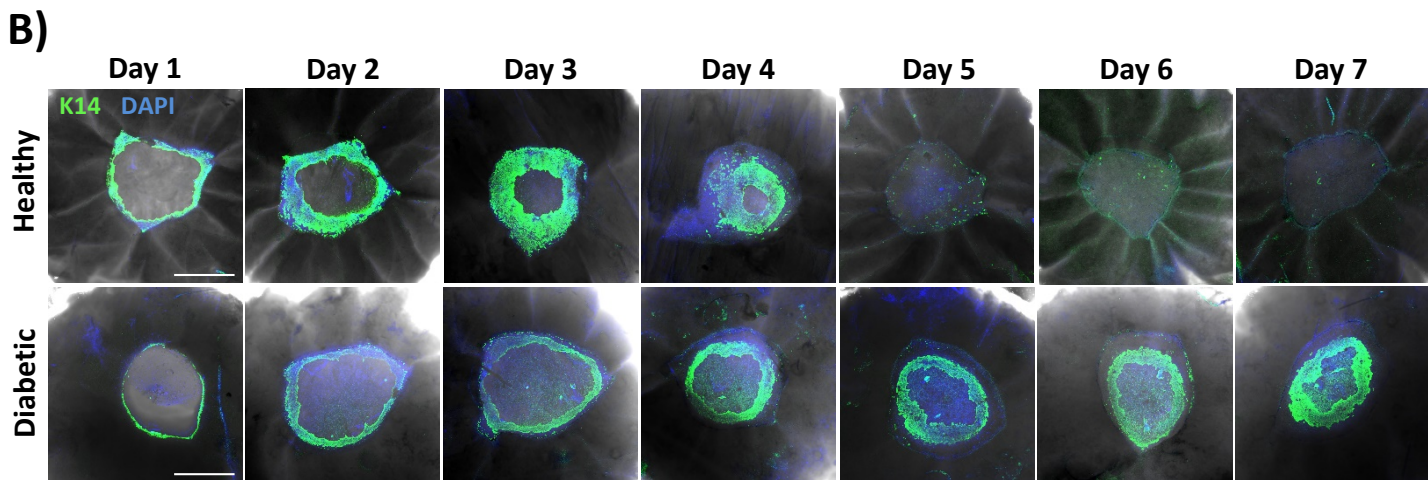
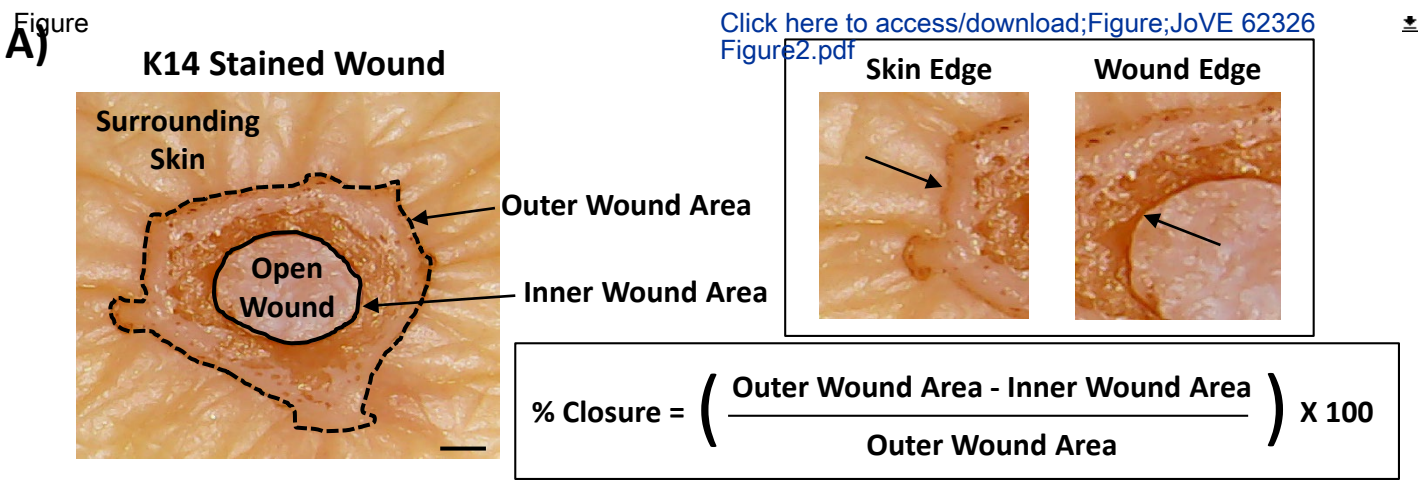
REFERENCES:

1. Lindholm, C., Searle, R. Wound management for the 21st century: combining effectiveness and efficiency. *International Wound Journal*. **13**, 5-15 (2016).
2. Guest, J. F. et al. Health economic burden that different wound types impose on the UK's National Health Service. *International Wound Journal*. **14** (2), 322-330 (2017).
3. Guest, J. F., Fuller, G. W., Vowden, P. Diabetic foot ulcer management in clinical practice in the UK: costs and outcomes. *International Wound Journal*. **15** (1), 43-52 (2018).
4. López-Valverde, M. E., et al. Perioperative and long-term all-cause mortality in patients with diabetes who underwent a lower extremity amputation. *Diabetes Research and Clinical Practice*. **141**, 175-180 (2018).
5. Wilkinson, H. N., Hardman, M. J. The role of estrogen in cutaneous ageing and repair. *Maturitas*. **103**, 60-64 (2017).
6. Frykberg, R. G., Banks, J. Challenges in the treatment of chronic wounds. *Advances in Wound Care*. **4** (9), 560-582 (2015).
7. Wilkinson, H. N., Hardman, M. J. Wound healing: cellular mechanisms and pathological outcomes. *Open Biology*. **10** (9), 200223 (2020).
8. Ansell, D. M., Holden, K. A., Hardman, M. J. Animal models of wound repair: Are they cutting it? *Experimental Dermatology*. **21** (8), 581-585 (2012).
9. Elliot, S., Wikramanayake, T. C., Jozic, I., Tomic-Canic, M. A modeling conundrum: murine models for cutaneous wound healing. *Journal of Investigative Dermatology*. **138** (4), 736-740 (2018).
10. Mazio, C. et al. Pre-vascularized dermis model for fast and functional anastomosis with host vasculature. *Biomaterials*. **192**, 159-170 (2019).

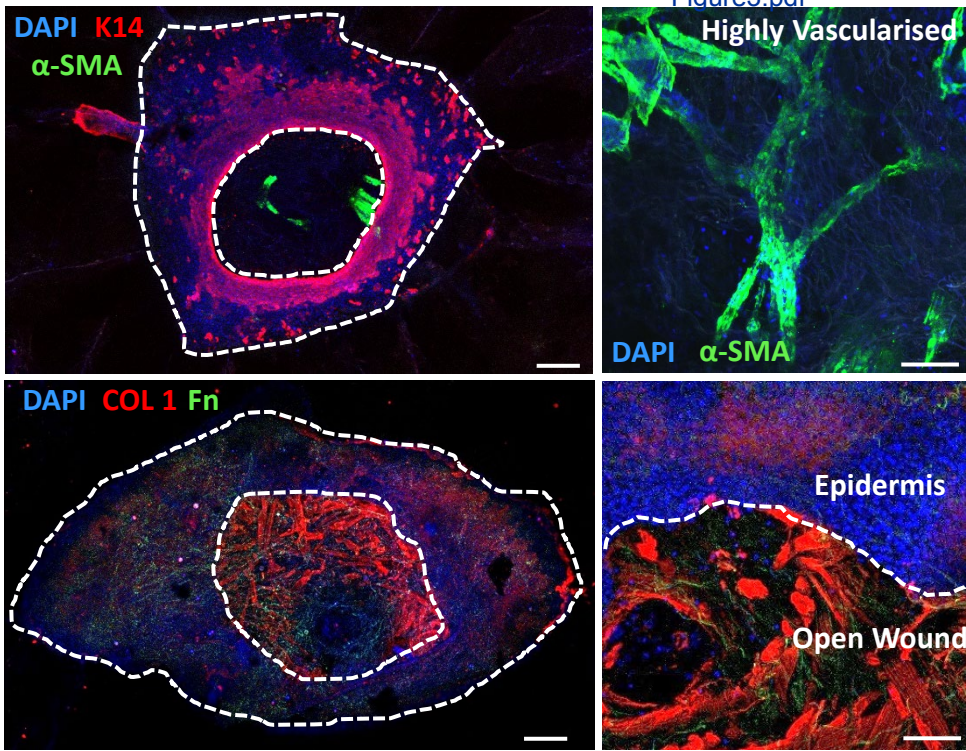
11. Wilkinson, H. N., Iveson, S., Catherall, P., Hardman, M.J. A novel silver bioactive glass elicits antimicrobial efficacy against *Pseudomonas aeruginosa* and *Staphylococcus aureus* in an ex vivo skin wound biofilm model. *Frontiers in Microbiology*. **9**, 1450 (2018).
12. Wilkinson, H. N. et al. Elevated local senescence in diabetic wound healing is linked to pathological repair via CXCR2. *Journal of Investigative Dermatology*. **139** (5), 1171-1181 (2019).
13. Wilkinson, H. N. et al. Tissue iron promotes wound repair via M2 macrophage polarization and the chemokine (CC motif) ligands 17 and 22. *The American Journal of Pathology*. **189** (11), 2196-2208 (2019).
14. Rhea, L., Dunnwald, M. Murine excisional wound healing model and histological morphometric wound analysis. *Journal of Visualized Experiments*. **162**, e61616 (2020).
15. Ansell, D. M., Campbell, L., Thomason, H. A., Brass, A., Hardman, M.J. A statistical analysis of murine incisional and excisional acute wound models. *Wound Repair and Regeneration*. **22** (2), 281-287 (2014).
16. Rizzo, A. E., Beckett, L. A., Baier, B. S., Isseroff, R. R. The linear excisional wound: an improved model for human ex vivo wound epithelialization studies. *Skin Research and Technology*. **18** (1), 125-132 (2012).
17. Olsson, M., et al. The humanistic and economic burden of chronic wounds: a systematic review. *Wound Repair and Regeneration*. **27** (1), 114-125 (2019).
18. Mendoza-Garcia, J., Sebastian, A., Alonso-Rasgado, T., Bayat, A. Optimization of an ex vivo wound healing model in the adult human skin: Functional evaluation using photodynamic therapy. *Wound Repair and Regeneration*. **23** (5), 685-702 (2015).
19. Brownhill, V. R., et al. Pre-clinical assessment of single-use negative pressure wound therapy during in vivo porcine wound healing. *Advances in Wound Care*. "In Press" 2020.
20. Diekmann, J., et al. A three-dimensional skin equivalent reflecting some aspects of in vivo aged skin. *Experimental Dermatology*. **25** (1), 56-61 (2016).
21. Vidal Yucha, S. E., Tamamoto, K. A., Nguyen, H., Cairns, D. M., Kaplan, D. L. Human skin equivalents demonstrate need for neuro-immuno-cutaneous system. *Advanced Biosystems*. **3** (1), 1800283 (2019).
22. Dijkgraaf, F. E. et al. Tissue patrol by resident memory CD8+ T cells in human skin. *Nature Immunology*. **20** (6), 756-764 (2019).
23. He, X., de Oliveira, V. L., Keijsers, R., Joosten, I., Koenen, H. J. Lymphocyte isolation from human skin for phenotypic analysis and ex vivo cell culture. *Journal of Visualized Experiments*. (110), e52564 (2016).
24. Pupovac, A. et al. Toward immunocompetent 3D skin models. *Advanced Healthcare Materials*. **7** (12), 1701405 (2018).
25. Ataç, B. et al. Skin and hair on-a-chip: in vitro skin models versus ex vivo tissue maintenance with dynamic perfusion. *Lab on a Chip*. **13** (18), 3555-3561 (2013).
26. Kim, J. J. et al. A microscale, full-thickness, human skin on a chip assay simulating neutrophil responses to skin infection and antibiotic treatments. *Lab on a Chip*. **19** (18), 3094-3103 (2019).
27. Jarret, C. et al. Development and characterization of a human Th17-driven ex vivo skin inflammation model. *Experimental Dermatology*. **29** (10), 993-1003 (2020).
28. Chen, J. L. et al. Metformin attenuates diabetes-induced tau hyperphosphorylation in vitro and in vivo by enhancing autophagic clearance. *Experimental Neurology*. **311**, 44-56 (2019).

- 705 29. Demirovic, D., Rattan, S. I. Curcumin induces stress response and hormetically modulates
706 wound healing ability of human skin fibroblasts undergoing ageing in vitro. *Biogerontology*. **12**
707 (5), 437-444 (2011).
- 708 30. Wilkinson, H. N., Hardman, M. J. Wound senescence: A functional link between diabetes
709 and ageing? *Experimental Dermatology*. **30** (1), 68-73 (2020).
- 710 31. Fisher, G. J. et al. Collagen fragmentation promotes oxidative stress and elevates matrix
711 metalloproteinase-1 in fibroblasts in aged human skin. *The American Journal of Pathology*. **174**
712 (1), 101-114 (2009).
- 713 32. Quan, T., Little, E., Quan, H., Voorhees, J. J., Fisher, G. J. Elevated matrix
714 metalloproteinases and collagen fragmentation in photodamaged human skin: impact of altered
715 extracellular matrix microenvironment on dermal fibroblast function. *Journal of Investigative*
716 *Dermatology*. **133** (5), 1362 (2013).
- 717

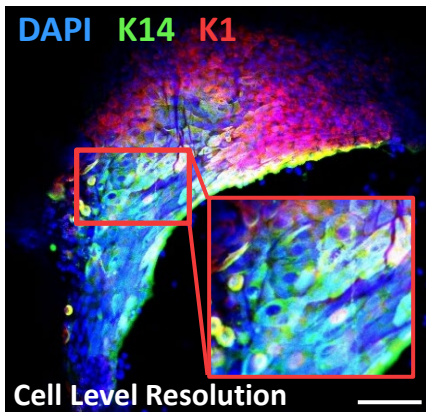




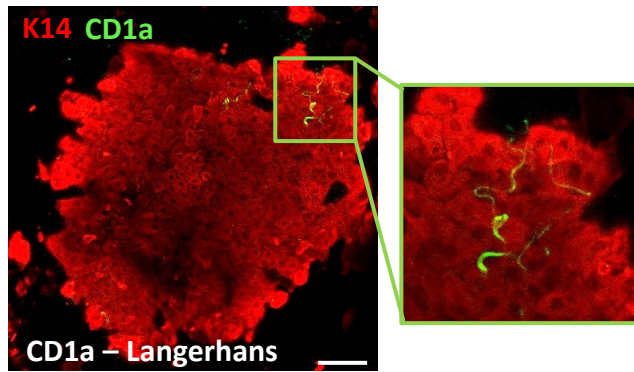
A)

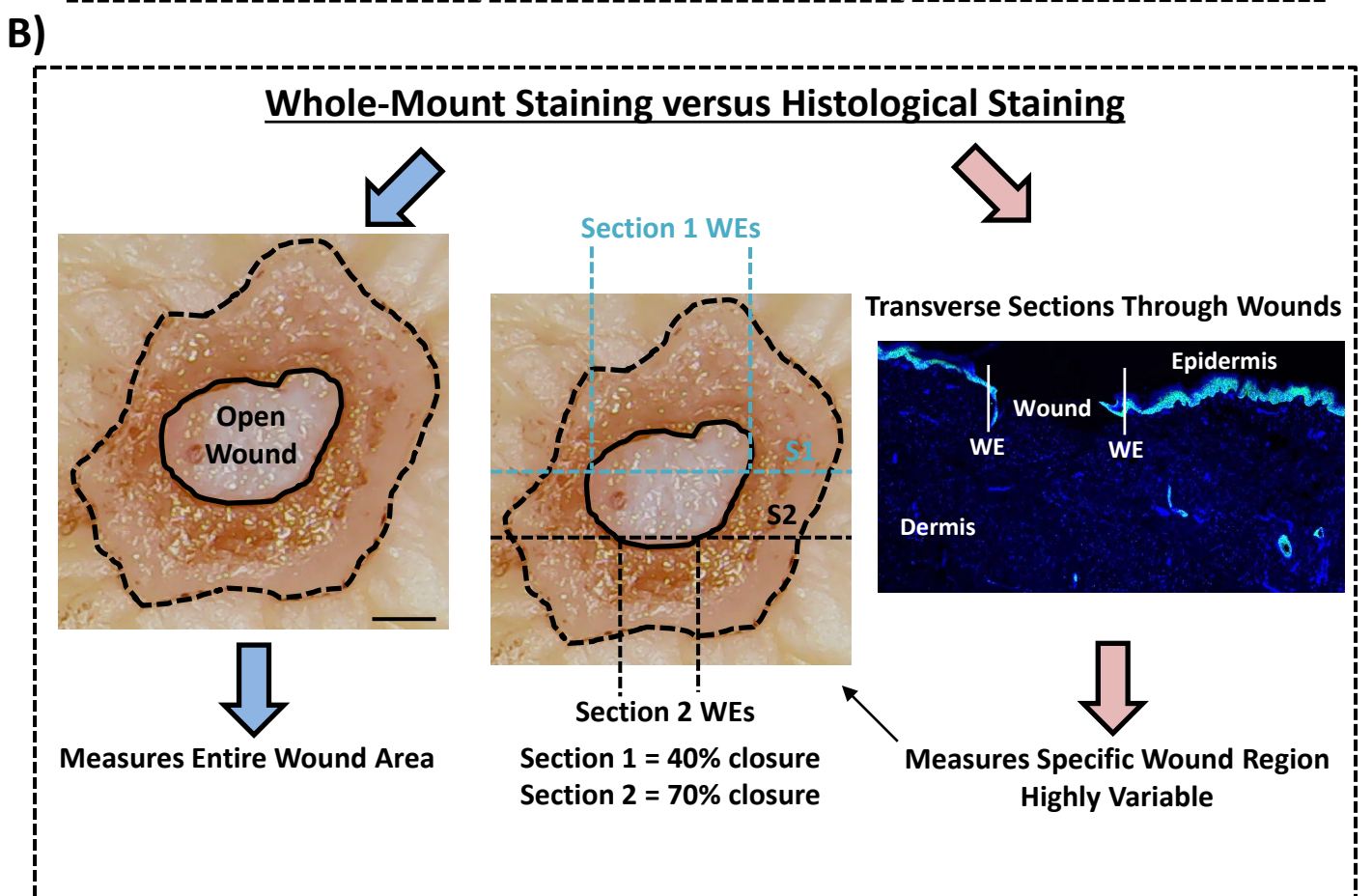
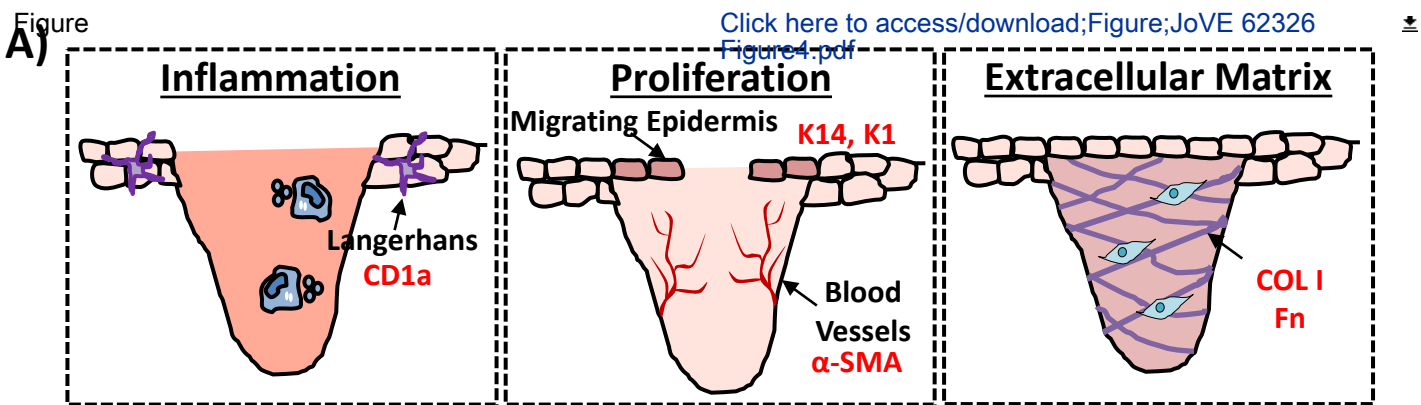


B)



C)





Name of Material/ Equipment	Company
50 mL Falcon Tubes	Falcon
1.5 ml TubeOne Microcentrifuge Tubes, Natural (Sterile)	Starlab
48-Well CytoOne Plate, TC-Treated	Starlab
Acetic Acid Glacial	Fisher Chemical
Alkyltrimethylammonium Bromide	Sigma-Aldrich
Anti-Alpha Smooth Muscle Actin Antibody [1A4]	Abcam
Anti-Collagen I Antibody	Abcam
Anti-Cytokeratin 14 Antibody [LL002]	Abcam
CD1A Antibody (CTB6)	Santa Cruz Biotechnology
DAPI (4',6-diamidino-2-phenylindole, dihydrochloride)	Thermo Fisher Scientific
Falcon 60mm Petri dishes	Falcon
Fibronectin Antibody (EP5)	Santa Cruz Biotechnology
Formaldehyde, Extra Pure, Solution 37-41%, SLR	Fisher Chemical
Gauze Swabs	Medisave
Gibco™ Antibiotic-Antimycotic Solution	Thermo Fisher Scientific
Gibco DMEM, high glucose, no glutamine	Thermo Fisher Scientific
Gibco Fetal Bovine Serum	Thermo Fisher Scientific
Gibco HBSS, no calcium, no magnesium	Thermo Fisher Scientific
Gibco L-Glutamine (200 mM)	Thermo Fisher Scientific
Hydrogen Peroxide	Sigma-Aldrich
ImageJ Software	National Institutes of Health
Invitrogen IgG (H+L) Cross-Adsorbed Goat anti-Mouse, Alexa Fluor 488	Thermo Fisher Scientific
Invitrogen IgG (H+L) Cross-Adsorbed Goat anti-Rabbit, Alexa Fluor 594	Thermo Fisher Scientific
Invitrogen LIVE/DEAD Viability/Cytotoxicity Kit, for mammalian cells	Thermo Fisher Scientific
Iris Forceps, 10 cm, Curved, 1x2 teeth	World Precision Instruments
Iris Scissors, 11 cm, Curved, SuperCut, Tungsten Carbide	World Precision Instruments
Iris Scissors, 11 cm, Straight, SuperCut, Tungsten Carbide	World Precision Instruments
Keratin 1 Polyclonal Antibody, Purified	Biolegend
Keratin 14 Polyclonal Antibody, Purified	Biolegend
LSM 710 Confocal Laser Scanning Microscope	Carl Zeiss
Merck Millipore Absorbent pads	Merck Millipore
Merck Millipore Nylon Hydrophilic Membrane Filters	Merck Millipore

Normal Goat Serum Solution
Phosphate Buffer Solution
Sodium Azide
Sodium Chloride
Sterilisation Pouches
Stiefel 2mm biopsy punches
Stiefel 6mm biopsy punches
Thermo Scientific Sterilin Standard 90mm Petri Dishes
Triton X-100
VECTASTAIN Elite ABC-HRP Kit, Peroxidase (Rabbit IgG)
Vector NovaRED Substrate Kit, Peroxidase (HRP)
Wireless Digital Microscope

Vector Laboratories
Sigma-Aldrich
Sigma-Aldrich
Fisher Bioreagents
Medisave
Medisave
Medisave
Thermo Fisher Scientific
Fisher Chemical
Vector Laboratories
Vector Laboratories
Jiusion

Catalog Number	Comments/Description
352070	<i>For skin washing</i>
S1615-5510	<i>For whole-mount staining</i>
CC7682-7548	<i>For whole-mount staining</i>
A/0400/PB15	<i>Part of fixative</i>
M7635	<i>Part of fixative</i>
ab7817	<i>Stains blood vessels</i>
ab34710	<i>Stains collagen</i>
ab7800	<i>Stains epidermis</i>
sc-5265	<i>Stains Langerhans cells</i>
62247	<i>Counterstain for cell nuclei</i>
353004	<i>Human ex vivo culture</i>
sc-8422	<i>Stains fibronectin</i>
F/1501/PB17	<i>Part of fixative</i>
CS1650	<i>To clean skin</i>
15240062	<i>Human ex vivo culture</i>
11960044	<i>Human ex vivo culture</i>
10500064	<i>Human ex vivo culture</i>
14170088	<i>Human ex vivo culture</i>
25030081	<i>Human ex vivo culture</i>
H1009-100ML	<i>For immunoperoxidase staining</i>
N/A	<i>For image analysis</i>
A11001	<i>Secondary antibody used depends on required fluorochromes and primary antibody</i>
A11012	<i>Secondary antibody used depends on required fluorochromes and primary antibody</i>
L3224	<i>For viability assessment of tissue</i>
15917	<i>To create wounds</i>
501264	<i>To create wounds</i>
501263	<i>To remove adipose tissue</i>
905201	<i>Stains epidermis</i>
905301	<i>Stains epidermis</i>
Discontinued	<i>For fluorescent imaging</i>
AP10045S0	<i>Human ex vivo culture</i>
HNWP04700	<i>Human ex vivo culture</i>

S-1000-20	<i>Animal serum used depends on secondary antibody</i>
P3619	<i>For wash buffer</i>
S2002	<i>For blocking buffer</i>
BP358-212	<i>Part of fixative</i>
SH3710	<i>To sterilise instruments</i>
BI0500	<i>For partial thickness wound</i>
BI2000	<i>For outer explant</i>
101VR20	<i>To prepare skin</i>
T/3751/08	<i>For wash buffer</i>
PK-6101	<i>For immunoperoxidase staining; HRP kit used depends on primary antibody</i>
SK-4800	<i>For immunoperoxidase staining</i>
N/A	<i>For brightfield imaging</i>

Name of Material / Equipme nt	Company	Catalog Number	ents/Description
---	---------	-------------------	------------------



Centre for Atherothrombosis and
Metabolic Disease

Hull York Medical School

Hull
University of Hull
Hull, HU6 7RX, UK

York
University of York
York, YO10 5DD, UK

www.hyms.ac.uk

4th December 2020

Dear Editor,

We are delighted that our enclosed manuscript '*Human Ex Vivo Wound Model and Whole-Mount Staining Approach to Accurately Evaluate Skin Repair*' has been favourably reviewed for publication in *The Journal of Visualized Experiments*. Please find below our rebuttal to the editorial and peer review comments.

Editorial comments:

Changes to be made by the Author(s):

1. Please take this opportunity to thoroughly proofread the manuscript to ensure that there are no spelling or grammar issues.
2. For in-text formatting, corresponding reference numbers should appear as numbered superscripts after the appropriate statement(s). Please ensure that citations follow an ascending chronology E.g. Line 534.
3. Line 103: Please specify the chemical(s) used.
4. Check lines 150-153. Are a total of 3 rinsing steps involved?
5. Line 186: Specify the humidity level.
6. Line 324: "Collect Z stacks.." instead of "Z stacks could be.."
7. Please include a single space between the quantity and its unit E.g. Line 377, 511: "3 mm" instead of "3mm".
8. Please do not use personal pronouns such as "we", "our" etc. in the protocol section.
9. Please include a single line spacing between the protocol steps. Furthermore, any text that cannot be written in the imperative tense may be added as a "Note." E.g.: Line 322-323
10. JoVE cannot publish manuscripts containing commercial language. This includes trademark symbols (™), registered symbols (®), and company names before an instrument or reagent. Please remove all commercial language from your manuscript and use generic terms instead. All commercial products should be sufficiently referenced in the Table of Materials. E.g. NovaRed, Alexa Fluor, Zeiss etc.

Response: We have now made the requested editorial changes to the manuscript. For point 4 we have also amended the text for clarification that there are 4 rinsing steps (2 x HBSS plus Abs, 1 x HBSS without antibiotics and 1 x DPBS).

Reviewers' comments:

Reviewer #1:

Manuscript Summary:

The submitted manuscript by Wilkinson et al., describes the development of an ex vivo 3D human skin wound healing model and whole mount staining approach, for the quantification of wound healing responses in skin. The validation and potential usefulness of this model were confirmed by the impaired 'wound' re-epithelialization observed in skin derived from diabetic patients compared to normal skin, akin to non-healing apparent in chronic wounds such as diabetic foot ulcers, which are a major issue for healthcare providers worldwide. Consequently, by using human skin samples, this model not only supports the 3Rs remit in biomedical research, but could further be utilised in future for the routine screening of new therapeutic entities, in terms of identifying their respective wound healing efficacies in promoting diabetic skin wound re-epithelialisation and their mechanisms of action. As a considerable limitation to current chronic wound therapy development involves the inadequate nature of existing 3D organotypic and ex vivo models, the current model described here may aid the successful translation of novel therapeutics into approved clinical use in future. Overall, this is an interesting and well-performed study, which builds on previous ex vivo wound healing model work published by the Authors. Thus, the manuscript is concise and generally well-written, whilst providing sufficient and straightforward to follow details on the methods and techniques used, in order to allow this experimental model to be reproduced in other laboratories. Consequently, I only have relatively limited number of minor comments for the Authors to address:-

1. Protocol (page 4). It would be useful if further details were included on the patients from which the non-diabetic and diabetic skin biopsies were collected? This is particularly true for the diabetic skin and how these patients were selected?

Response: We thank the reviewer for raising this point. Non-diabetic skin was collected from patients undergoing routine surgery (mean age = 68). Diabetic skin was selected from donors who had established type II diabetes and a history of ulceration (mean age = 81). We have updated the text to include this information.

2. Related to this, it appears that the Human Skin Growth Media used was high glucose DMEM (presumably at 25 mM concentrations)? Could the Authors clarify whether both non-diabetic and diabetic ex vivo cultures were maintained in high glucose DMEM, as I would assume that non-diabetic cultures were maintained in more normal glucose concentrations (i.e. 5.5 mM glucose-containing DMEM)? If this is the case, details of the normal glucose medium needs to be included here. if not, could the Authors justify why both non-diabetic and diabetic ex vivo cultures were maintained in high glucose DMEM?

Response: All cultures were maintained in high glucose DMEM. The rationale for this is to allow evaluation of intrinsic differences in cellular behaviour rather than differences that may in fact be due to culturing each group in different glucose levels. Indeed, the fact that we see a difference between non-diabetic and diabetic skin when both are cultured in the same media conditions demonstrates that there are intrinsic cellular differences in the diabetic skin that contribute to delayed healing. It would be interesting to explore the role of these intrinsic versus extrinsic factors in skin culture in the future.

3. Protocol (page 6). Could the Authors please provide details on to what extent 'wound' formation by punch biopsy can vary between patient donors and skin sites used? i.e. Could this lead to potential problems with variability in wound healing responses within experimental groups and between different experimental groups?

Response: The reviewer raises an important point. In our extensive experience, we do observe donor differences at the point of wounding. For example, aged skin generally requires less force to generate wounds and skin with significant stretch marks can be

challenging to use. However, in general, most skin is suitable for ex vivo wounding. We have not directly compared the healing potential of ex vivo skin derived from different body sites, but we have successfully used skin from different body sites for ex vivo wound healing studies.

As with all human research, there is inherent variability between donors. There are also many external factors that can influence ex vivo healing, a significant one being the time from surgical tissue collection to ex vivo wound set up. For this very reason, we never split treatment groups across multiple donors/sites. We have updated the discussion text to include some of this information.

4. Results (page 11). The Authors very nicely show enhanced wound closure and re-epithelialization in normal skin 'wounds' over 7 days in culture. However, have the Authors extended these cultures beyond 7 days and if so, does the model show any evidence of keratinocyte differentiation/stratification within this air/medium interface model, once wound repair is complete?

Response: We have not extended ex vivo skin cultures beyond 7 days as we primarily use this model to evaluate wound re-epithelialisation. We agree that it would be interesting in the future to explore keratinisation/stratification of the re-epithelialised tissue.

5. Blood vessel assessment (page 13 and Figure 3). Could the Authors please explain the choice of α -SMA as a blood vessel marker, over more established angiogenic markers, e.g. CD31?

Response: We have optimised the α -SMA monoclonal from Abcam for both histological and whole-mount wound samples. We thank the reviewer for the suggestion of exploring CD31 and will do so in the future.

6. Figures 3 and 4 (pages 13 and 14). Could the Authors please clarify which ex vivo skin samples were used to generate the data presented in Figures 3 and 4? I presume that these are derived from normal skin ex vivo cultures, but need to be confirmed within the text and the Figure legends. Related to this, could the Authors explain why data for both normal and diabetic skin were not included here, as characterisation of these additional parameters would provide added strength to the ex vivo model, in terms of the additional differences between normal and diabetic skin wound healing observed.

Response: The data presented in Figure 3 and 4 pertains to normal (non-diabetic) skin. We have updated both text and Figure legends to clarify this. We agree that detailed characterisation of the ex vivo diabetic healing model is important, but we feel this is beyond the scope of this current methods paper. Our approach was to include diabetic skin data in Figure 2 to demonstrate the utility of the ex vivo model to show differences in overall wound closure. By contrast, the focus of Figure 3 was to illustrate the diversity of markers that can be evaluated. Nevertheless, we thank the reviewer for this suggestion and we plan to address it in the future.

Reviewer #2:

Manuscript Summary:

This study describes a human ex vivo wound model and whole mount staining for the performance of high throughput re-epithelialization measurements. The manuscript is well written and touches on the main strength and weaknesses of the model.

Minor Concerns:

The authors did not elaborate on the possibilities to use these samples for traditional histological analyses that could complement their whole mount evaluation. Can this be done? If so, it may be interesting to indicate how. It would have been interesting to know if findings on the whole mount correlates with findings on sections.

Response: It is absolutely possible to process (wax or OCT) and section whole-mount samples for histology. This allows direct comparison of whole-mount measured versus histological measured healing. We have not attempted to perform immunohistochemistry on samples that have been whole-mount stained, but in theory this should be possible. We have updated the manuscript discussion to emphasise the possibility of combining whole-mount staining with subsequent traditional histological analysis.

What is the minimum size of human tissue required for these studies? Understanding that it will vary from one experimental design to another, it may be useful for the audience to have an appreciation of how much tissue is needed, considering that human samples may not be trivial to acquire.

Response: We agree with the point the reviewer makes that access to human skin is not trivial. For a time course experiment as shown (using n=6 per group), a 5x5 cm piece of skin should suffice when using a biopsy diameter of 6mm.

Figure 2, panel D, last panel on the right. It is indicated: Loss of KI4. This is somewhat inaccurate, as KI4 is not loss, but the visualization of KI4 is impaired because of lack of penetration of the antibody. At a minimum, it should say Loss of KI4 staining. To this point, careful wording is warranted when discussing this issue in the manuscript, to make sure that it is the loss of the staining, and not the loss of the protein that is occurring with healing.

Response: We thank the reviewer for making this point. We have now carefully amended the figure and text for clarification.

Figure 3, panels B and C are hard to interpret. What is the orientation? What are we looking at?

Response: Both panels B and C are ex vivo wounds imaged in the same orientation as A (i.e. wounded epidermis side up). Panel B illustrates keratin localisation in migrating epidermis at the edge of the wound at high power. Panel C shows Langerhans cell staining (CD1a) in the epidermis of a fully re-epithelialised wound.

Figure 4, panel A, extracellular panel: I would recommend using COL I and Fn .

Response: We have amended the text as suggested.

Figure 4, panel B. By itself, this panel is hard to understand. One suggestion would be to not separate the two parts of the panel, but rather having one common title (whole-mount staining versus histological staining), with two downward arrows to their respective staining. The "measures entire wound area" and "measures specific..." should be placed at the same level to highlight the contrast. "Measures specific wound region orientation and sectioning variability" is confusing, may be could say "Measures Specific Wound Region Highly Variable" .

Response. We thank the reviewer for their insight and we have amended the panel as suggested.

Minor details:

2mm and 6mm punches: throughout the manuscript, there is no space between the number and the unit. Typically, the scientific language would require a space. Is it common rule to omit the space in this case?

P4, line 95, the use of "theatre" is awkward

P5, line 134, igG should be capitalized

P10, line 333, "petri" should be capitalize

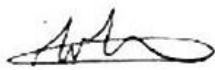
P12, line 408, "wound KI4 levels" is awkward

P15, line 518, should say "reduced"

Response: We thank the reviewer for highlighting these points and we have made amendments as suggested (red text where appropriate).

Thank you again for considering our work.

Yours Sincerely,



Dr Holly N Wilkinson
Lecturer in Wound Healing
Hull York Medical School
T: +44 (0)1482 461879
E: h.n.wilkinson@hull.ac.uk